(2)

ARMY RESEARCH LABORATORY

The Burning Rate Behavior of Pure Nitrocellulose Propellant Samples

Frederick W. Robbins
Theresa Keys

ARL-TR-82

March 1993

NOTICES

REPORT DOCUMENTATION PAGE	Form Approved OMB No. 0704-0188

1. AGENCY USE ONLY (Leave blank)	2. REPORT DATE	3. REPORT TYPE AND DATES COVERED
	March 1993	Final, Jan 79 - Dec 81

4. TITLE AND SUBTITLE

The Burning Rate Behavior of Pure Nitrocellulose Propellant Samples

5. FUNDING NUMBERS

PR: 1L162618AH80

6. AUTHOR(S)

Frederick W. Robbins and Theresa Keys

7. PERFORMING ORGANIZATION NAME(S) AND ADDRESS(ES)

8. PERFORMING ORGANIZATION REPORT NUMBER

9. SPONSORING/MONITORING AGENCY NAME(S) AND ADDRESS(ES)

U.S. Army Research Laboratory
ATTN: AMSRL-OP-CI-B (Tech Lib)
Aberdeen Proving Ground, MD 21005-5066

10. SPONSORING/MONITORING AGENCY REPORT NUMBER

ARL-TR-82

11. SUPPLEMENTARY NOTES

12a. DISTRIBUTION/AVAILABILITY STATEMENT

Approved for public release; distribution is unlimited.

12b. DISTRIBUTION CODE

13. ABSTRACT *(Maximum 200 words)*

Closed bomb firings have been conducted to determine the burning rate behavior of pure nitrocellulose (NC) gun propellants. Samples produced and tested included nitration levels of 12.02, 12.65, 13.11%, in both zero and seven-perforated cylindrical geometries. A sample containing basic lead carbonate was also included. Burning rates derived from the closed bomb tests were compared to strand burner data measured on samples extruded from the same NC batches. The burning rate plots for the pure NC samples show the characteristic slope changes of propellants with additives.

14. SUBJECT TERMS	15. NUMBER OF PAGES
interior ballistics; closed bomb tests; strand burner tests; pressure	32
	16. PRICE CODE

17. SECURITY CLASSIFICATION OF REPORT	18. SECURITY CLASSIFICATION OF THIS PAGE	19. SECURITY CLASSIFICATION OF ABSTRACT	20. LIMITATION OF ABSTRACT
UNCLASSIFIED	UNCLASSIFIED	UNCLASSIFIED	UL

INTENTIONALLY LEFT BLANK.

ACKNOWLEDGMENTS

The authors wish to thank T. C. Smith, S. E. Mitchell, and C. G. Irish for their helpful discussions and suggestions. (Note: The U.S. Army Ballistic Research Laboratory was deactivated on 30 September 1992 and subsequently became part of the U.S. Army Research Laboratory (ARL) on 1 October 1992.)

INTENTIONALLY LEFT BLANK.

TABLE OF CONTENTS

INTENTIONALLY LEFT BLANK.

LIST OF FIGURES

LIST OF TABLES

INTENTIONALLY LEFT BLANK.

1. INTRODUCTION

In performing any gun interior ballistic calculations, the burning rate or the rate of regression of the burning propellant is one of the most significant input parameters (Haukland and Burnett 1972). The burning rate is used in interior ballistics computer codes with the propellant density and the geometry of the propellant grains to compute the mass generation rate. The mass generation rate is integrated to determine the instantaneous mass of propellant burned. Using an equation of state to calculate the average pressure in the gun chamber and a pressure gradient equation, the projectile base pressure is calculated. With the projectile base pressure known, the acceleration, velocity, and travel of the projectile can be determined.

The closed bomb, which is most frequently used to generate experimental burning rate data for gun propellants, is a closed vessel in which propellant is burned and the resulting pressure is monitored as a function of time. Theoretically, the burning rate at all pressures, up to the maximum pressure attained in the bomb, can be determined. Propellants have, in general, a monotomically increasing burning rate as a function of pressure. When the logarithms of the burning rates are plotted vs. the logarithms of the pressures, one obtains straight-line segments which frequently have distinctly different slopes. This behavior is difficult to explain with either flamespread or variable thermodynamics.

The work described in this report was conducted to establish a database for propellant grains containing only nitrocellulose (plus the residual solvents necessarily remaining from the processing). It was also hoped to determine if the additives frequently used in gun propellants, such as basic lead carbonate, diphenyl amine, or potassium sulfate, caused or affected the changes in the slopes of the burning rate curves. The work was planned to include various nitrogen levels of nitrocellulose (NC) without any additives and at least one sample with basic lead carbonate for comparison. Both closed bomb and strand burning rate tests were included in the test program. Production, tests, and analysis were performed at the Naval Ordnance Station, Indian Head, MD, between 1979 and 1981.

2. EXPERIMENTAL APPROACH

The three NC nitrogen levels selected for evaluation were those most frequently used in conventional gun propellants, nominally, 12.0, 12.6, and 13.15%. The actual levels of the NC used for the propellant samples were 12.02, 12.65, and 13.11%. Two grain configurations, zero- and seven-perforation right

circular cylinders, were selected for the closed bomb testing, and solid strands were used for the strand burning rate tests. In addition to the "pure" NC samples, an additional 12.65% nitrogen sample was made with 0.85% of basic lead carbonate, which was processed in the seven-perforation right circular cylinder granulation.

The propellant samples were manufactured using the conventional processing techniques of mixing with solvent in a horizontal, sigma-blade mixer, extrusion, and cutting to length. All samples for each nitrogen level were processed using the same batch of NC and the same ratios and levels of solvents; the solvent levels did vary from one nitrogen level to another. The grains and strands were dried very slowly in order to minimize shrinkage, maximize straightness, and produce a relatively nonporous, smooth surface texture.

The zero-perforation grains were extruded to a nominal 0.318 cm diameter and cut to a length of 0.64 cm; the seven-perforation grains had nominal dimensions of 0.64 cm in diameter and 1.3 cm in length, and had perforations diameters of 0.038 cm. The strands were nominally 0.64 cm in diameter. The actual grain dimensions and residual solvent levels are given in Table 1. It should be noted that the 12.02% nitrogen level samples were not as smooth as the samples of the two other nitrogen levels and had some uncolloided NC dispersed throughout the grains. It is felt that the surface area definition for solvent-processed extruded grains, because of shrinkage and rough surfaces, is not as correct as for solventless extruded propellant grains, but burning rate trends can probably be captured.

The thermodynamic properties of the propellants used in the data reduction for the closed bomb tests were calculated with the Blake code (Freedman 1974) (Table 1). Values for the 0.25 g/cm^3 loading density were chosen. No variable thermodynamic properties were used in the calculations.

The igniter system for the closed bomb tests consisted of an M100 match boosted with 1.1 g of Dupont 700x. A series of five shots was conducted for each grain type in the 182.4-cm^3 closed bomb at ambient temperature. The first two firings were at reduced charge weights to determine a charge weight which will give a nominal peak pressure of 310 MPa. The pressure data were digitized at 25-µs intervals and stored on magnetic tape. Burning rates were then computed from the pressure history with two different programs. The first, CIBOM (Wynne 1976), is a program which computes the time rate of change of mass burned (dm/dt) from the time rate of change of pressure (dP/dt). Using least squares, dP/dt is obtained by fitting the pressure data to a cubic polynomial and evaluating the differentiated

Table 1. Values for Experimental Propellant Samples

Mix No.	Geometry	Dia. (cm)	Length (cm)	Dia. of outer perf. (cm)	Dia. of inner perf. (cm)	Distance between perf. centers (cm)	NC (%)	Water (%)	Ethyl alcohol (%)	Ether (%)	BLAKE code output: Flame temp. (K)	BLAKE code output: Mole-cular wt.	BLAKE code output: Co-volume cm^3 (g)	gamma	Loading density (g/cm^3)	Heat capacity at constant volume (cal/g·K)
13.11% Nitrogen Level																
599	0-Perf. Grains	0.325	0.645	—	—	—	96.2	1.0	0.00	2.80	2,974	23.953	1.0018	1.2412	0.25	0.344
599	Strands	—	—	—	—	—	95.2	1.3	0.00	3.50	—	—	—	—	—	—
597	7-Perf. Grains	0.635	1.347	0.041	0.046	0.168	96.3	1.6	0.00	2.10	3,011	24.225	0.9926	1.2383	0.25	0.344
12.65% Nitrogen Level																
600	0-Perf. Grains	0.315	0.620	—	—	—	94.9	1.5	1.08	2.52	2,710	23.129	1.0172	1.2503	0.25	0.343
618	Strands	—	—	—	—	—	93.9	1.7	1.32	3.08	—	—	—	—	—	—
618	7-Perf. Grains	0.663	1.232	0.051	0.056	0.168	94.7	1.4	1.17	2.73	2,688	23.017	1.0207	1.2515	0.25	0.343
598*	7-Perf. Grains	0.632	1.280	0.029	0.030	0.165	94.95	1.7	0.75	1.75	2,789	23.721	0.9994	1.2459	0.25	0.340
12.01% Nitrogen Level																
619	0-Perf. Grains	0.330	0.610	—	—	—	94.1	1.8	2.87	1.23	2,433	22.388	1.0345	1.2603	0.25	0.341
619	Strands	—	—	—	—	—	93.7	1.9	3.08	1.32	—	—	—	—	—	—
602	7-Perf. Grains	0.623	1.234	0.042	0.043	0.168	94.4	2.1	2.45	1.05	2,468	22.569	1.0280	1.2581	0.25	0.341

* 0.85% basis lead carbonate.

polynomial. The second, FRBOM (Robbins and Horst 1976), computes dm/dt by calculating the mass at a pressure and the mass at some higher pressure and equating dm/dt to the change in the calculated mass burned in an integral number of sample time intervals ($\Delta m/\Delta t$). Both programs fit, by a least squares analysis, the burn rate-pressure data to a power law in specified pressure ranges.

The strand burner tests were conducted at ten pressures, ranging from 3.5 to 55.2 MPa. Testing was limited by the capability of the existing strand burner facility to a maximum pressure of 55.2 MPa. An average of three or four shots at each pressure was used to determine the burning rate.

3. RESULTS

The burning rate descriptions, coefficient and exponent, for straight-line segments are given in Table 2. Burning rates calculated with CIBOM and FRBOM differ by approximately 0.5%. The plots cannot be distinguished from each other when overlaid, except that one is smoother because of smoothing techniques intrinsic to the separate programs (Figure 1). The difference in tail-off is caused by different slivering routines of the programs.

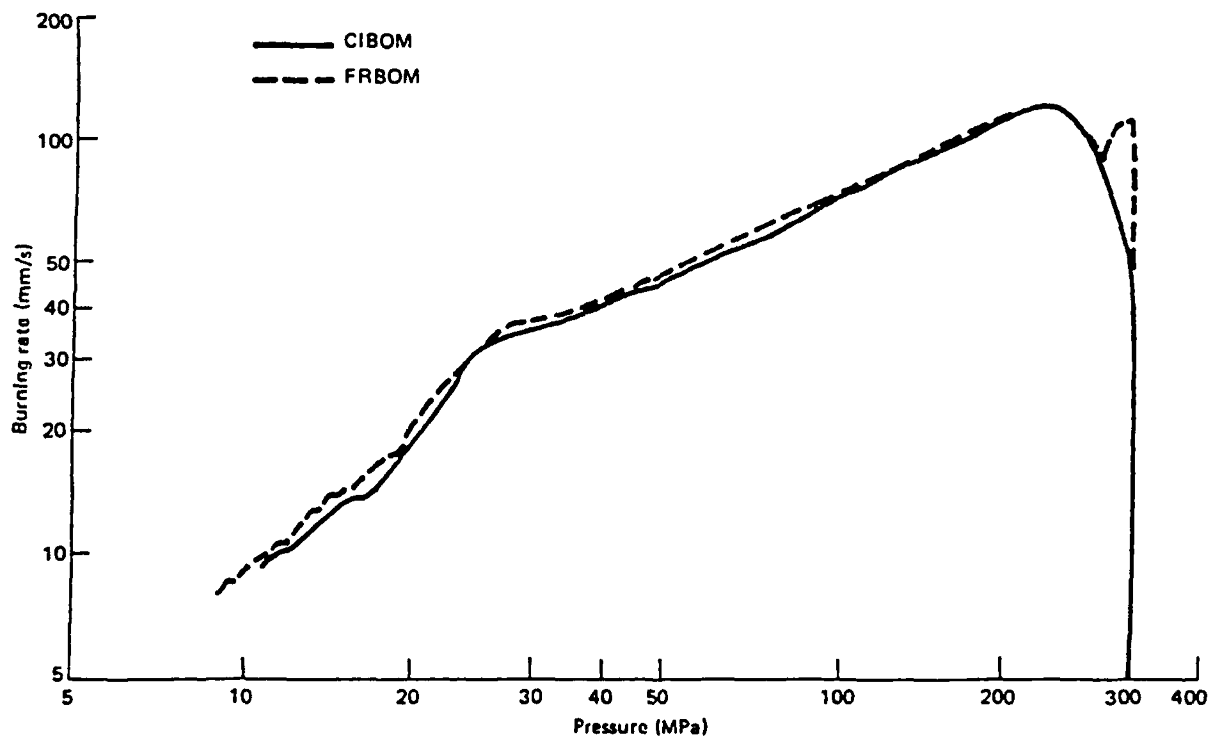

Note: (12.65% Nitrocellulose and 0.85% Basic Lead Carbonate; Seven-Perforation)

Figure 1. Comparison of Burning Rates Determined by CIBOM and FRBOM.

Table 2. Firing Data

Shot No.	Charge Weight (g)	Pressure Range (MPa) From	Pressure Range (MPa) To	FRBOM Burning Rates a^a	FRBOM Burning Rates n	CIBOM Burning Rates a^a	CIBOM Burning Rates n
Mix 599; 13.11% Nitrogen; Zero-Perforation							
5521	35.3029	27.60	34.47	19.9471	0.2040	22.2969	0.1734
		52.40	199.95	1.4973	0.8748	1.4972	0.8780
5522	39.9057	27.60	34.47	21.5340	0.1620	24.4027	0.1298
		52.40	206.84	1.6250	0.8614	1.6783	0.8576
5523	46.0018	27.60	34.47	17.2457	0.2203	16.0490	0.2466
		52.40	206.84	1.7483	0.8382	1.8358	0.8315
5524	46.0002	27.60	34.47	11.6321	0.3265	10.2240	0.3698
		52.40	206.84	1.7283	0.8393	1.8358	0.8315
5525	46.0011	27.60	34.47	19.4128	0.1828	17.7892	0.2132
		52.40	206.84	1.6471	0.8479	1.7375	0.8415
Mix 597; 13.11% Nitrogen; Seven-Perforation							
5570	34.9940	27.60	34.47	2.6290	0.8136	2.8944	0.7886
		52.40	137.90	6.1477	0.5950	6.4684	0.5858
5571	39.9552	27.60	34.47	3.7167	0.7206	3.5571	0.7384
		52.40	151.68	5.4104	0.6279	5.7231	0.6180
5572	46.4200	27.60	34.47	8.3865	0.4811	6.5257	0.5590
		52.40	206.84	5.3967	0.6265	5.8204	0.6131
5573	46.4245	27.60	34.47	5.9056	0.5846	6.9375	0.5434
		52.40	206.84	5.4425	0.6269	5.8668	0.6136
5574	46.4562	27.60	34.47	5.0472	0.6293	5.3546	0.6176
		52.40	206.84	5.2287	0.6361	5.6132	0.6237

Table 2. Firing Data (Continued)

Shot No.	Charge Weight (g)	Pressure Range (MPa)		FRBOM Burning Rates		CIBOM Burning Rates	
		From	To	a[a]	n	a[a]	n
Mix 600; 12.65% Nitrogen; Zero-Perforation							
5547	35.0068	27.60	34.47	6.5287	0.3897	6.7893	0.3823
		51.71	199.95	1.2311	0.8356	1.1790	0.8491
5550	40.0058	27.60	34.47	4.1997	0.5160	4.5261	0.4991
		51.71	220.63	1.1259	0.8576	1.1496	0.8564
5551	48.0030	27.60	34.47	6.3103	0.4245	6.2799	0.4314
		51.71	275.79	1.3643	0.8212	1.4191	0.8162
5552	48.0015	27.60	34.47	7.1999	0.3845	8.6308	0.3367
		51.71	275.79	1.3287	0.8308	1.3903	0.8249
5553	48.0045	27.60	34.47	4.9753	0.4870	4.9213	0.4955
		51.71	275.79	1.2859	0.8385	1.3353	0.8340
Mix 618; 12.65% Nitrogen; Seven-Perforation							
5554	34.9793	27.60	34.47	7.3827	0.4219	7.7595	0.4126
		41.37	137.90	4.9339	0.5598	5.1807	0.5512
5555	37.9560	27.60	34.47	7.1000	0.4411	9.4756	0.3616
		41.37	158.58	3.6138	0.6364	3.9677	0.6193
5556	49.0344	27.60	34.47	9.6098	0.3537	8.7089	0.3872
		41.37	206.84	3.2867	0.6618	3.5329	0.6491
5557	49.0202	27.60	34.47	13.9378	0.2505	13.8855	0.2568
		41.37	206.84	3.4195	0.6533	3.6646	0.6413
5560	49.0970	27.60	34.47	7.2511	0.4361	8.4079	0.3984
		41.37	206.84	3.2748	0.6618	3.5262	0.6488

Table 2. Firing Data (Continued)

Shot No.	Charge Weight (g)	Pressure Range (MPa) From	Pressure Range (MPa) To	FRBOM Burning Rates a[a]	FRBOM Burning Rates n	CIBOM Burning Rates a[a]	CIBOM Burning Rates n
Mix 598; 12.65% Nitrogen + Lead Carbonate; Seven-Perforation							
5575	34.7507	27.60	34.47	2.1856	0.7884	1.9063	0.8322
		51.71	68.95	2.1821	0.7784	2.3445	0.7641
5576	39.8752	27.60	34.47	4.4870	0.5834	4.5961	0.5803
		51.71	144.79	3.0956	0.6916	3.2712	0.6814
5577	48.0219	27.60	34.47	7.7972	0.4416	7.2113	0.4673
		51.71	206.84	3.2674	0.6794	3.4706	0.6684
5600	48.1474	27.60	34.47	6.2027	0.5109	5.1741	0.5688
		51.71	206.84	3.1391	0.6862	3.3592	0.6737
5601	48.4281	27.60	34.47	7.6102	0.4482	7.0883	0.4737
		51.71	206.84	3.1654	0.6858	3.3969	0.6729
Mix 619; 12.02% Nitrogen; Zero-Perforation							
5563	35.0000	20.68	34.47	3.9600	0.4713	3.8449	0.4849
		34.47	48.26	1.5056	0.1032	1.5682	0.0971
		52.40	172.37	0.6013	0.9261	0.5902	0.9344
5564	50.0027	20.68	34.47	3.1799	0.5579	3.1504	0.5669
		34.47	48.26	1.5248	0.1179	1.4829	0.1312
		52.40	282.69	0.7357	0.8870	0.7638	0.8850
5565	51.5062	20.68	34.47	3.4988	0.5234	3.5160	0.5283
		34.47	48.26	9.8150	0.2311	10.0196	0.2271
		52.40	282.69	0.7015	0.9008	0.7423	0.8930
5566	51.7021	20.68	34.47	2.4746	0.6153	2.1904	0.6605
		34.47	48.26	9.7078	0.2339	10.2737	0.2247
		52.40	282.69	0.7729	0.8794	0.8162	0.8717
5567	51.6990	20.68	34.47	2.5912	0.6110	2.4560	0.6327
		34.47	48.26	15.1008	0.1215	15.0201	0.1283
		52.40	282.69	0.7400	0.8918	0.7780	0.8848

Table 2. Firing Data (Continued)

Shot No.	Charge Weight (g)	Pressure Range (MPa)		FRBOM Burning Rates		CIBOM Burning Rates	
		From	To	a[a]	n	a[a]	n
Mix 602; 12.02% Nitrogen; Seven-Perforation							
5602	35.3960	27.60	34.47	1.4499	0.8327	1.5009	0.8263
		34.47	68.95	6.6948	0.3910	6.9655	0.3841
		68.95	137.90	1.8271	0.6998	1.9277	0.6899
5603	40.4598	27.60	34.47	4.1592	0.5201	4.6199	0.4946
		34.47	68.95	6.0552	0.4161	6.1781	0.4149
		68.95	151.68	1.7437	0.7119	1.5366	0.7452
5604	52.1113	27.60	34.47	9.1854	0.3173	8.3647	0.3493
		52.40	89.63	4.3762	0.5076	4.6649	0.4963
		89.63	206.84	1.0995	0.8178	1.2159	0.7990
5605	52.0176	27.60	34.47	12.3612	0.2305	11.4309	0.2583
		52.40	89.63	4.0788	0.5249	4.2515	0.5188
		89.63	206.84	0.9707	0.8440	1.0374	0.8321
5606	52.0420	27.60	34.47	6.7997	0.4078	7.5536	0.3831
		52.40	89.63	3.4053	0.5679	3.5751	0.5602
		89.63	206.84	0.9811	0.8418	1.0861	0.8226

[a] The units of "a" are mm/(s·MPa^n).

The variation from shot to shot (Figure 2) was determined to be approximately 1% at the higher pressure range (207 MPa) and 2% at the lower pressure range (28 MPa) as calculated from values of the coefficient (a) and exponent (n) in Table 2.

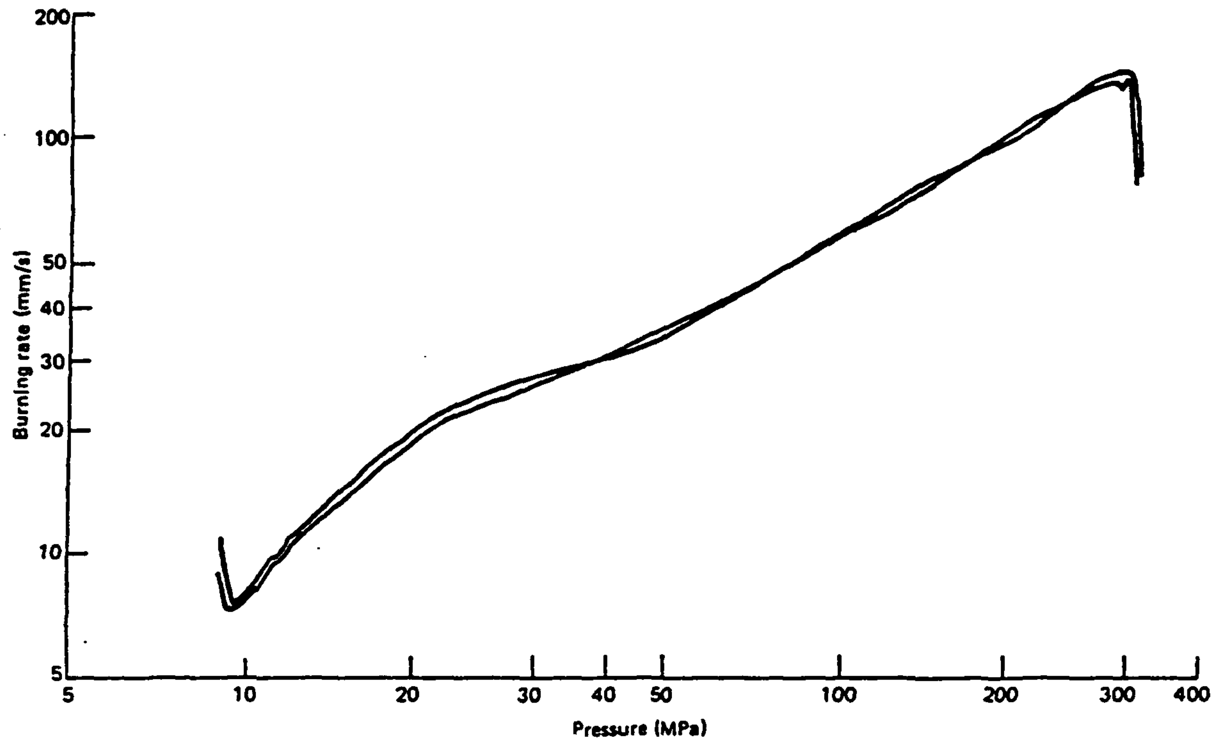

Note: (12.65% Nitrogen; Zero-Perforation)

Figure 2. Shot-to-Shot Variations in Burning Rate Curves.

3.1 Burning Rate as a Function of NC Nitrogen Content. A composite of representative burning rate curves for the zero- and seven-perforation grains for the three nitrogen levels are given in Figure 3. Select comparisons are given in Figures 3a–e. As would be expected, for both grain geometries, the burning rates are higher for the higher nitrogen level grains. The curves on each figure appear parallel, though the high-pressure portions of the 12.02% NC curves have a slightly larger burning rate exponent than the higher nitrogen NC curves (0.89–0.83 for the zero-perforation and 0.84–0.64 for the seven-perforation grains).

It is evident that the curves of all three nitrogen levels have slope breaks (Figures 3a and 3b) and at least three separate sections. Further, for each grain geometry the slope breaks occur in nearly the same

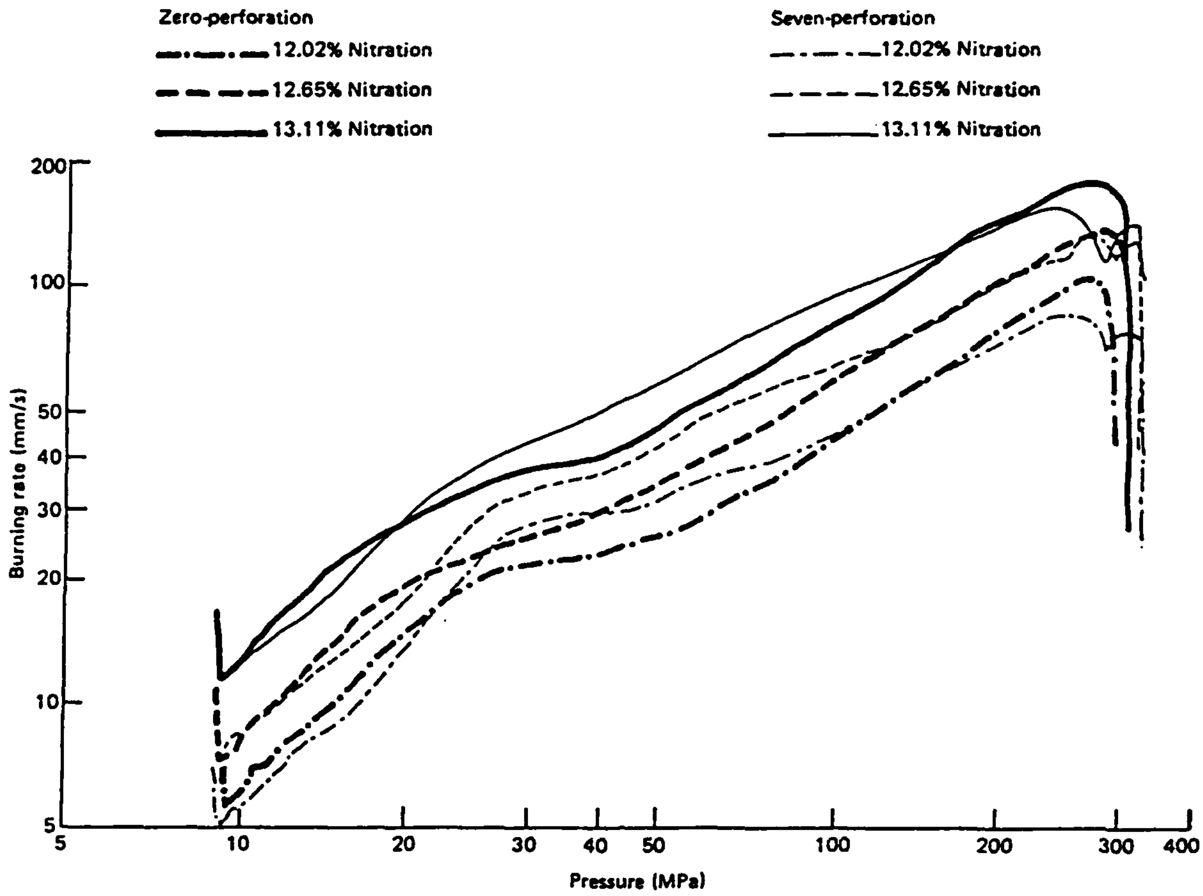

Figure 3. Burn Rate Curves for Zero- and Seven-Perforation Grains With Different Nitrogen Levels.

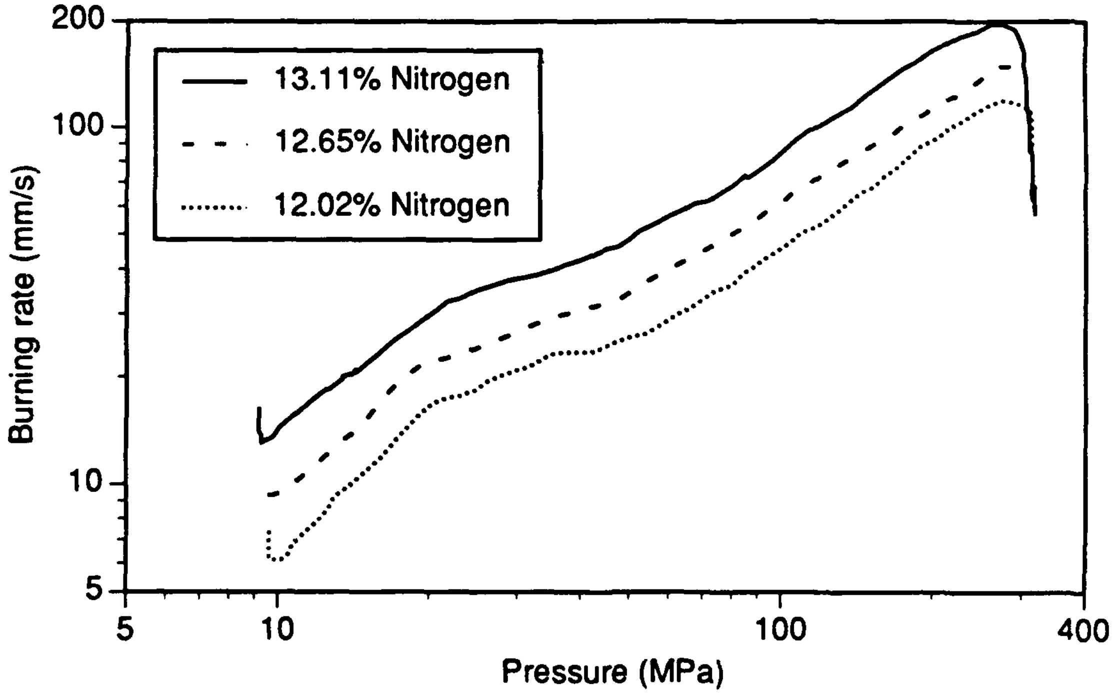

Figure 3a. Burn Rate Curves for Grains With Zero Perforations and Various Nitrogen Levels.

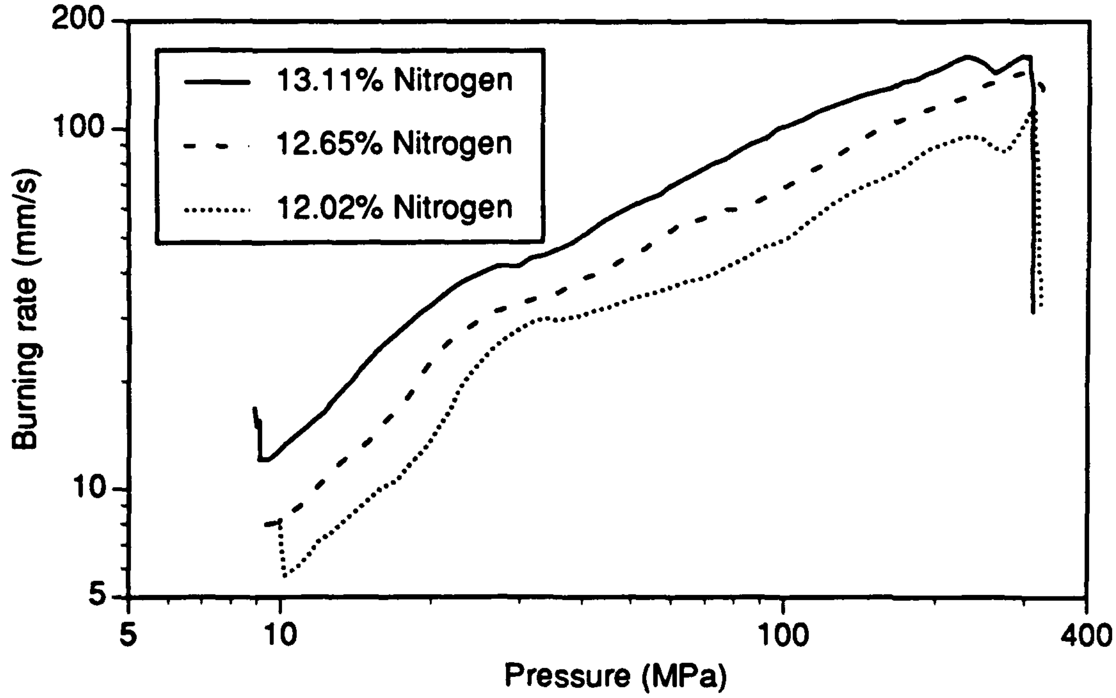

Figure 3b. Burn Rate Curves for Grains With Seven Perforations and Various Nitrogen Levels.

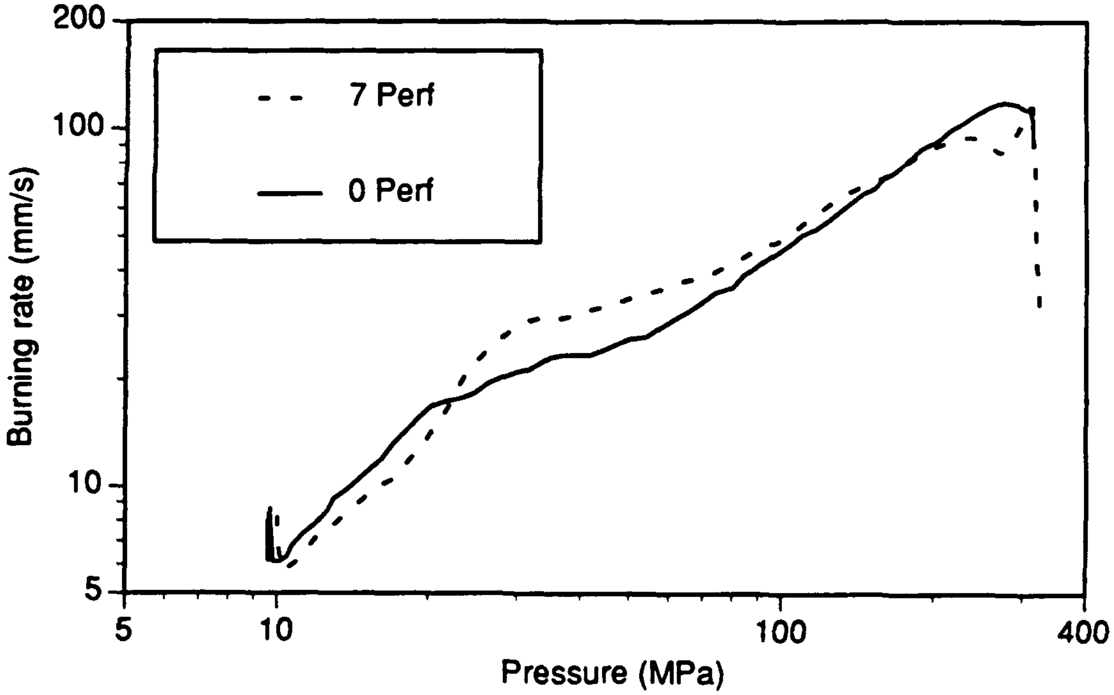

Figure 3c. Burn Rate Curves for Grains With Seven and Zero Perforations and 12.02% Nitrogen.

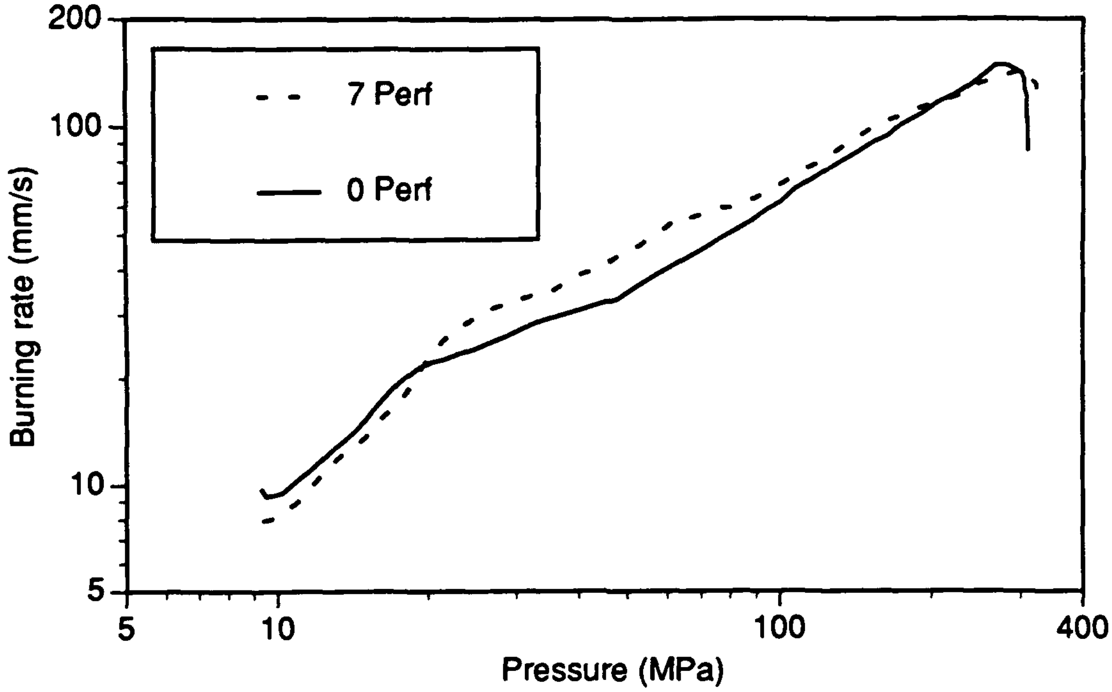

Figure 3d. Burn Rate Curves for Grains With Seven and Zero Perforations and 12.65% Nitrogen.

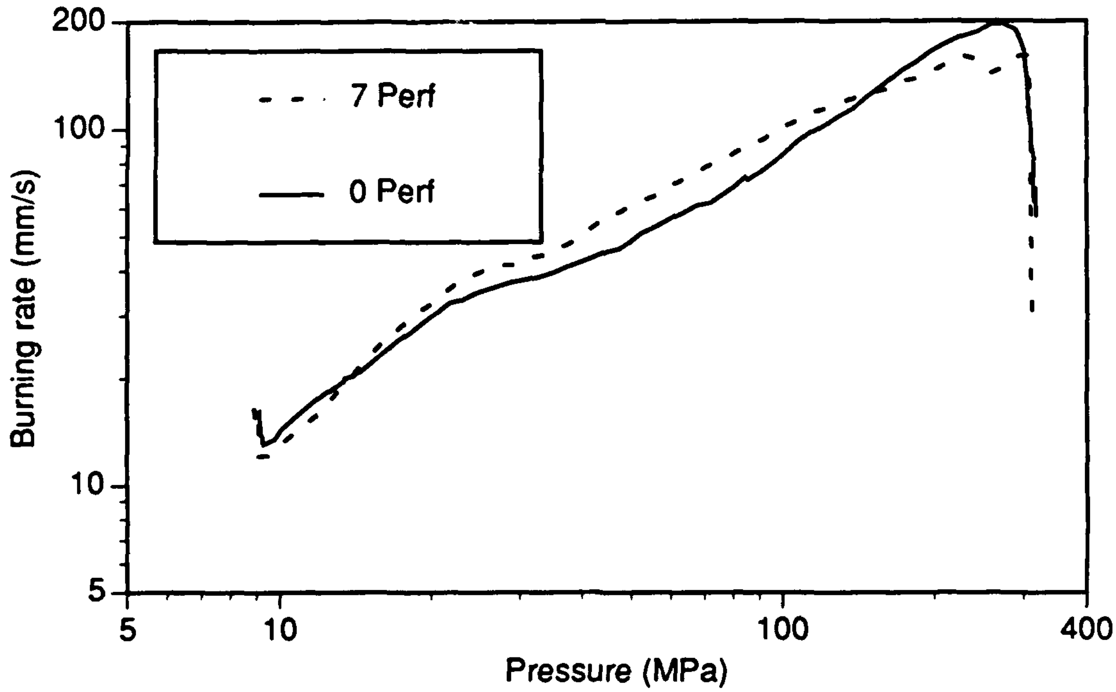

Figure 3e. Burn Rate Curves for Grains With Seven and Zero Perforations and 13.11% Nitrogen.

pressure range for all nitrogen levels. For the zero-perforation grains, the first major break occurs around 20 MPa and the second major break occurs at 35 to 50 MPa with some suggestion that the second one occurs at the lower end of the range for the higher nitrogen levels. For the seven-perforation grains, the breaks are at 21 to 28 MPa and at 34 to 70 MPa. However, the break in the 12.02% nitrogen level tends to be much higher for the seven-perforation grains (up to 90 MPa) than for the zero-perforation grains (up to 48 MPa).

The humps at high pressure for the seven-perforation grains are caused by smoothing through the pressure-time curve at slivering with a cubic polynomial. Even though the program (FRBOM) has an exact solution for the surface function routine, the cubic equation cannot adjust itself well enough to compensate for the discontinuous dp/dt at that point.

The parallelism of the different segments of the burning rate vs. pressure curve would suggest that rationalization of the burning rates, as proposed by Irish (1979) and supported by data of Riefler (Riefler and Lowery 1974) and Grollman (Grollman and Nelson 1977) is a viable technique which should allow easy ranking of propellants with respect to their burning rates. In Table 3, three exponents have been chosen and the corresponding coefficients have been calculated for the seven-perforation propellant. The ranking according to nitrogen level is evident with a higher coefficient for higher nitrogen levels. In Figure 4, the coefficients for the three nitrogen levels and the two grain geometries, assuming a burning rate exponent of 0.8, are plotted vs. adiabatic flame temperature (which is proportional to nitrogen level with minor perturbations due to volatile levels). This figure shows the usefulness of having one number to characterize a whole section of a burning rate curve.

3.2 Comparison of Zero- and Seven-Perforation Grain Burning Rates. The burning rate data for zero- and seven-perforation grains are compared for the three nitrogen levels in Figures 3c–e. All seven-perforation burning rates above 21 MPa are higher than those of the corresponding zero-perforation grains of the same nitrogen level, but the rates merge at about 210 MPa just before slivering occurs. This would suggest that, since the volatile levels did not vary greatly for each nitrogen level and there was no pattern of difference in volatile levels in the two grain geometries, the elevation of the burning rate for the seven-perforation grains is a function of the perforations.

If the apparent burning rate augmentation is a function of the perforations, a higher mass generation rate inside the perforations is suggested as the cause. This, in turn, suggests a higher pressure inside the

Table 3. Rationalized Burning Rate Coefficients (For the Equation $r = aP^n$)

Mix No.	Nitrogen Level (%)	Water (%)	Total Volatiles (%)	No. of Perf.	T_f (K)	$\frac{\Sigma \ln r}{N}$ [ln(mm/s)]	$\frac{\Sigma \ln P}{N}$ (MPa)	N	Burning Rate Coefficient mm/(s·MPa^n)			
									n = .85[a]	n = .80[a]	n = .80[b]	n = .75[a]
599	13.11	1.0	4.1	0	2,974	4.5284	4.7236	618	1.671	2.116	2.148	2.680
600	12.65	1.3	4.4	0	2,710	4.4046	4.9474	1,147	1.221	1.563	1.665	2.002
619	12.02	2.8	6.9	0	2,433	4.1240	4.9535	1,580	0.917	1.175	1.158	1.505
597	13.11	1.0	4.0	7	3,011	4.6305	4.6675	424	1.941	2.451	2.216	3.095
618	12.65	1.6	5.6	7	2,688	4.2198	4.5571	680	1.414	1.776	1.625	2.230
602	12.02	1.5	5.2	7	2,468	3.9390	4.6523	821	0.985	1.243	1.222	1.568
598[c]	12.65	1.2	4.7	7	2,789	4.3508	4.6518	600	1.487	1.876	1.802	2.368

[a] From Irish: $a = EXP\,[(\Sigma \ln r)/N - n \cdot (\Sigma \ln P)/N]$

[b] From Grollman and Nelson: $a = 4.19 \times 10^{-4}\,(T_f - 1{,}800)n^{-9.4}$ [mm/(s · MPa^n)].

[c] With 0.85% basic lead carbonate.

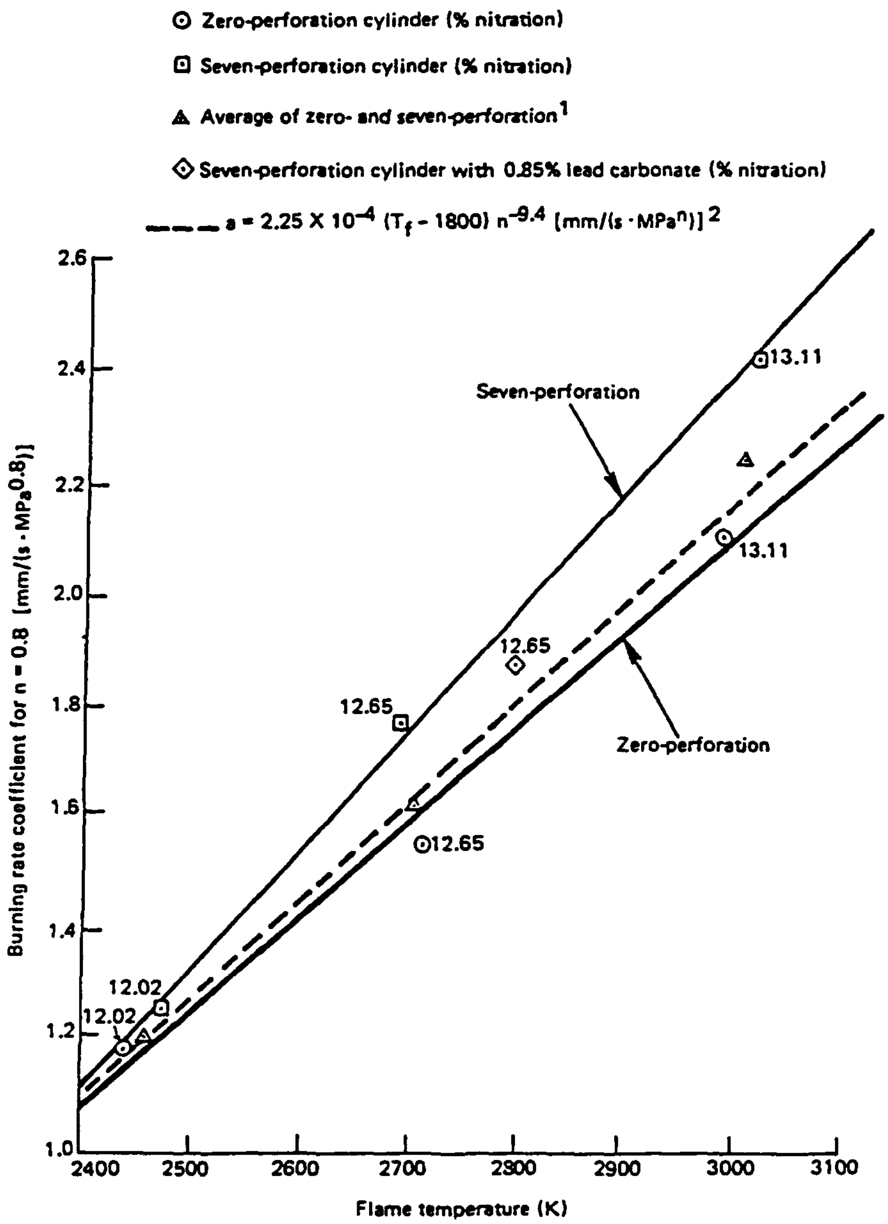

[1] Burning averaged using $\frac{\sum \log P}{N}$, $\frac{\sum \log r}{N}$, N.

[2] From Grollman and Nelson.

Note: For a Burning Rate Exponent of 0.8.

Figure 4. Burning Rate Coefficient vs. Flame Temperature.

perforations or an increase in the surface area by expansion or splitting. (There is evidence, however, that grains do not split [Naval Ordnance Station 1979a, 1979b; Robbins and Bingham 1981].) This hypothesis should be studied with a computer model to determine what pressure differential must be maintained in that pressure regime to cause the apparent enhancement in burning rate.

This geometry effect was not noted in a similar study with NOSOL, an easily ignited double-base propellant (Mitchell and Horst 1976). The data reduction technique and closed bomb collection procedure for the NOSOL and pure NC samples were the same, but the NOSOL perforations were two to three times larger than those of the pure NC samples.

3.3 Strand Burner Data. The strand burning data are given in Table 4 and plotted in Figure 5. The corresponding zero-perforation grain closed bomb burning rates are provided in Figure 5. The strand data have not been corrected for their total volatile content. Corrected data would be slightly higher on the graphs since all solvent levels are higher for the strands than for the grains. Notwithstanding uncorrected strand data, it is considered noteworthy that the strand data exhibit the same trends with respect to nitrogen content (including characteristic slope breaks) as the closed bomb data.

The strand burning rate data at low pressures are lower than that extrapolated from closed bomb data using mid-pressure ranges. The technique of extrapolation closed bomb data from mid-pressure range to low pressures is often the procedure used in determining the burning rate input for two-phase flow interior ballistics codes such as NOVA (Gough 1977) where flamespread is modeled. It has been assumed that the first high slope section between 5 and 20 MPa is a combination of flamespread and the intrinsic burning rate of the propellant and, therefore, should not be used in a flamespread model. The low pressure burning rate data obtained from the strand burner tests suggest that extrapolation of closed bomb data to low pressures may, however, involve incorrect assumptions about the influence of flamespread. Simulations of the 5-inch, 54-caliber gun system were made with the NOVA code to illustrate the effect of the low-pressure burning rate data. Two computations were made with only one difference: one extrapolated the closed bomb mid-pressure burning rate data to low pressures (as has been done traditionally) and the other used the low-pressure burning rate data from the closed bomb. The resulting pressure-time curves for two gauge locations (case base and case mouth) and the associated pressure difference (ΔP) curve are compared in Figure 6. The use of the actual low pressure data has the effect of reducing the magnitude of the calculated pressure difference and causing a longer ignition delay.

Table 4. Strand Burning Test Data

Pressure (MPa)	Burning rates at 25° C (cm/s)	Average burning rates (cm/s)
Mix 619; 12.02% Nitrogen NC		
3.45	0.292, 0.358, 0.300	0.318
6.89	0.569, 0.569, 0.589	0.577
10.34	[a], 0.759, [a], 0.826	0.792
13.79	0.925, 0.927, 1.036, 1.156	1.011
20.68	1.400, [a], 1.435, 1.278	1.372
27.58	1.748, 1.524, 1.692, 1.699	1.666
34.47	2.670, 2.261, 2.479, 2.583	2.499
41.37	2.101, 2.182, 1.986, 2.139	2.103
48.26	2.642, 2.250, 2.291, 2.162	2.337
55.16	2.344, 3.078, 3.124, 2.731	2.819
Mix 618; 12.65% Nitrogen NC		
3.45	0.310, 0.315, 0.315	0.312
6.89	0.640, 0.612, 0.617	0.622
10.34	0.866, 0.848, 0.907	0.872
13.79	1.100, 1.107, 1.107	1.105
20.68	1.565, 1.600, 1.575	1.580
27.58	1.872, 1.887, 1.902	1.887
34.47	2.146, 2.159, 2.106	2.136
41.37	2.377, 2.334, 2.375	2.362
48.26	2.670, 2.647, 2.662	2.659
55.16	3.005, 3.028, 3.094	3.043
Mix 599; 13.11% Nitrogen NC		
3.45	0.427, 0.439, 0.409, 0.417	0.424
6.89	0.813, 0.836, 0.846	0.831
10.34	1.128, 1.135, 1.133	1.133
13.79	1.461, 1.461, 1.473	1.466
20.68	1.925, 2.007, 1.979	1.971
27.58	2.405, 2.492, 2.423	2.441
34.47	2.835, 3.272, 2.880	2.995
41.37	3.213, 3.368, 3.203	3.261
48.26	4.115, 4.158, 4.069	4.115
55.16	4.234, 4.216, 4.257	4.237

[a] Test strand flashed.

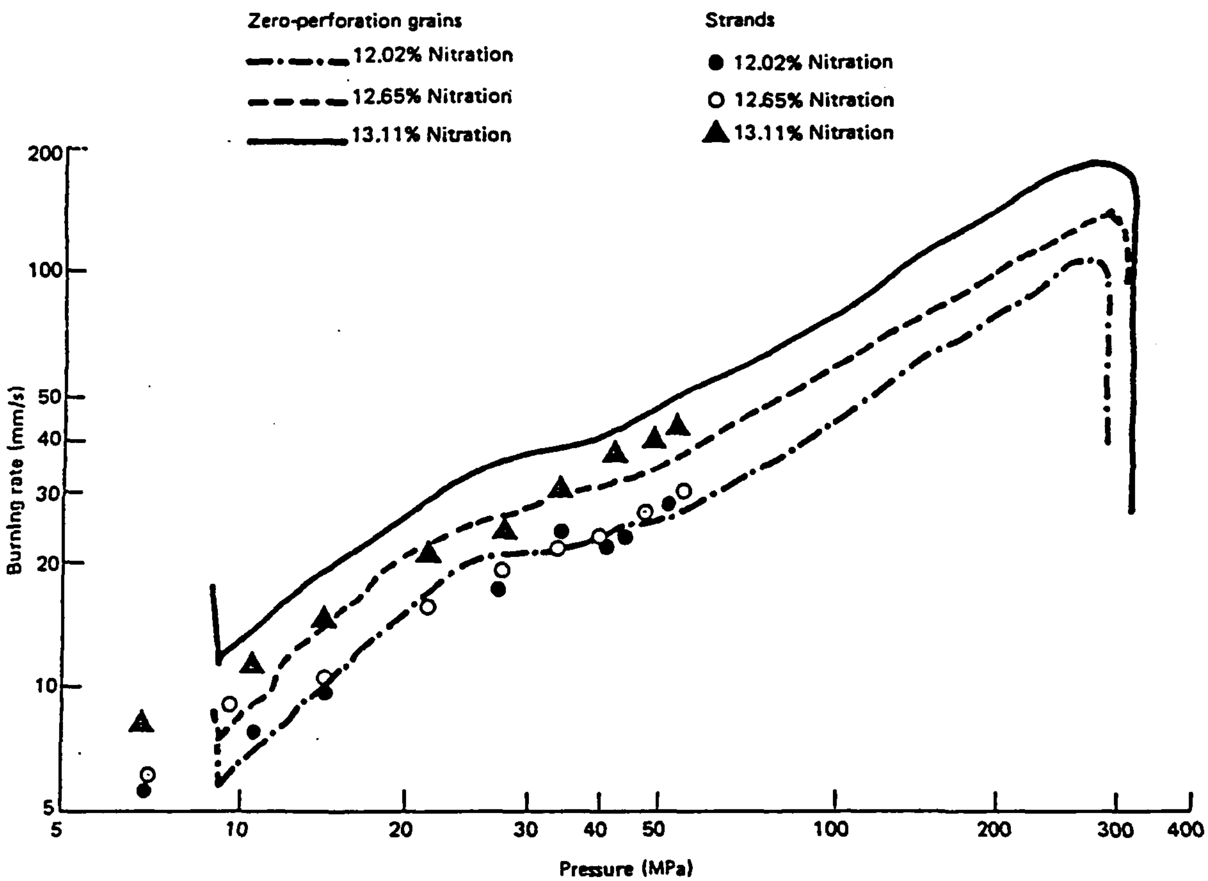

Figure 5. Comparison of Burning Rates of Strands and Zero-Perforation Grains.

4. CONCLUSIONS AND RECOMMENDATIONS

The following conclusions resulted from the study:

(1) A database of burn rate equations has been presented for pure NC grains for three nitration levels and for NC with a basic lead carbonate additive for a 12.65% nitrogen level.

(2) The burning rate plots for pure NC show the characteristic slope changes of propellants with additives.

(3) The data suggest an enhanced burning rate associated with the presence of perforations in the grain.

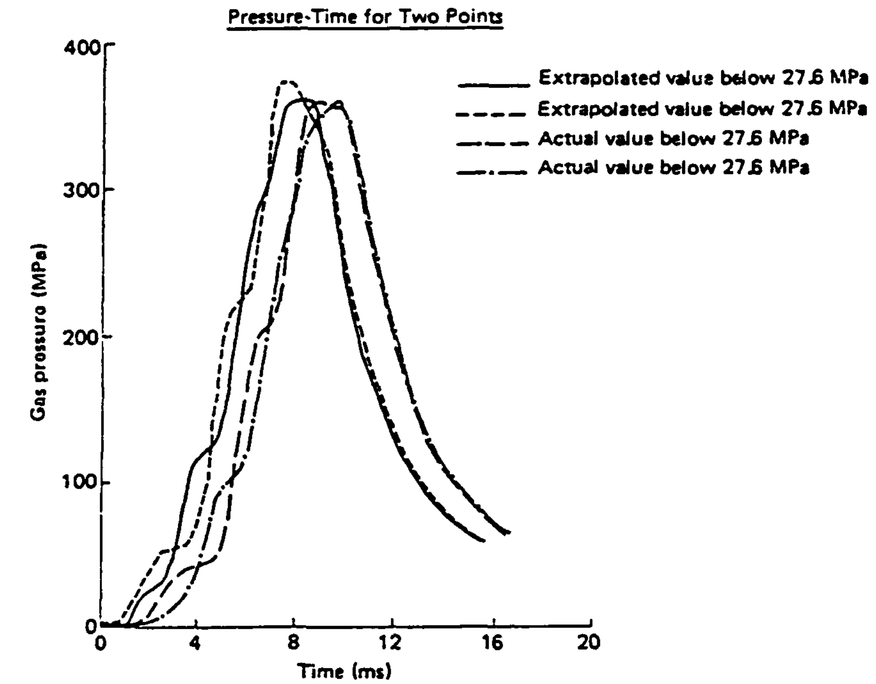

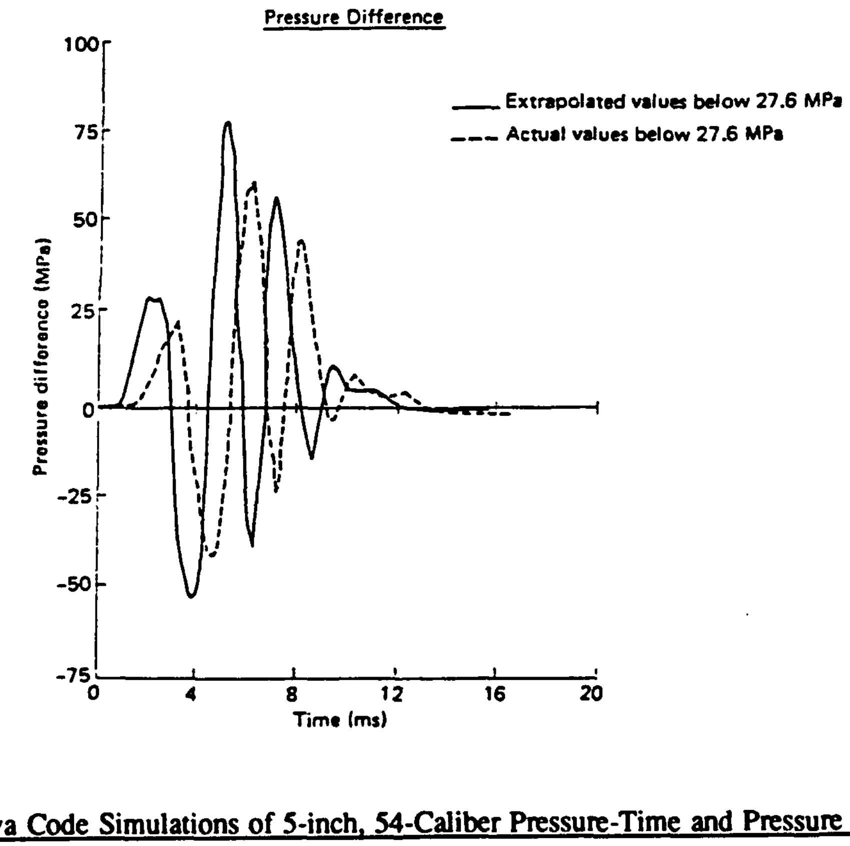

Figure 6. Nova Code Simulations of 5-inch, 54-Caliber Pressure-Time and Pressure Difference Curves.

(4) Two data reduction computer programs were run on the same data with no significant difference noted in calculated burn rates between the programs.

(5) The low-pressure strand burning rate data agree with the low-pressure closed bomb burning rate data and suggest that the low-pressure section of the closed bomb burning rate curve is significant.

(6) The maximum difference in calculated burning rates from one closed bomb firing to another of the same propellant at the same loading density was in the order of 2%.

The following recommendations are offered:

(1) In a continuation of the study, high-pressure strand burning data should be obtained and the effects of solvent level should be studied.

(2) The use of measured low pressure burn rate data is recommended to provide improved simulation of the flamespread event with two phase flow interior ballistic codes.

5. REFERENCES

Freedman, E. "A Brief Users Guide for the BLAKE Program." BRL-IMR-249, U.S. Army Ballistic Research Laboratory, Aberdeen Proving Ground, MD, July 1974.

Gough, P. S. "Numerical Analysis of a Two-Phase Flow With Explicit Internal Boundaries." IHCR 77-5, Paul Gough Associates, Inc., Portsmouth, NH, 1 April 1977.

Grollman, B. B., and C. W. Nelson. "Burning Rates of Standard Army Propellants in Strand Burner and Closed Chamber Tests." BRL-MR-2775, U.S. Army Ballistic Research Laboratory, Aberdeen Proving Ground, MD, August 1977.

Haukland, A. C., and W. M. Burnett. "Sensitivity of Interior Ballistic Performance to Propellant Thermochemical Parameters." Proceedings of the Tri-Service Gun Propellant Symposium, vol. 1, par. 7.3-1, Picatinny Arsenal, Dover, NJ, 11–13 October 1972.

Irish, C. G., Jr. "An Attempt to Rationalize NACO Propellant Burning Rate Descriptions." Proceedings of the 16th JANNAF Combustion Meeting, Monterey, CA, CPIA Publication 308, vol. 1, pp. 399–415, December 1979.

Mitchell, S. E., and A. W. Horst. "Comparative Burning Rate Study." Proceedings of the 13th JANNAF Combustion Meeting, Monterey, CA, CPIA Publication 308, vol. 1, pp. 383–404, September 1976.

Naval Ordnance Station. Technology Quarterly, Gun Ammunition Propulsion, July–September 1979, Indian Head, MD, pp. 29–30, 28 February 1979a.

Naval Ordnance Station. Technology Quarterly, Gun Ammunition Propulsion, July–September 1979, Indian Head, MD, pp. 3–4, 31 August 1979b.

Riefler, D. W., and D. S. Lowery. "Linear Burn Rates of Ball Propellants Based on Closed Bomb Firings." BRL Contract Report No. 172, U.S. Army Ballistic Research Laboratory, Aberdeen Proving Ground, MD, August 1974.

Robbins, F. W., and R. P. Bingham. "A Study of the Burning Characteristics of Multiperforated Gun Propellant Grains." IHTR 697, U.S. Army Ballistic Research Laboratory, Aberdeen Proving Ground, MD, 10 March 1981.

Robbins, F. W., and A. W. Horst. "Numerical Simulation of Closed Bomb Performance Based on BLAKE Code Thermodynamic Data." IHMR 76-295, U.S. Army Ballistic Research Laboratory, Aberdeen Proving Ground, MD, 29 November 1976.

Wynne, G. J. "Y Bomb—A Computer Program for the Collection, Storage, and Processing of Pressure-Time Data From Propellant Burned in a Closed Bomb." IHTR, April 1976.

INTENTIONALLY LEFT BLANK.

No. of Copies	Organization
2	Administrator Defense Technical Info Center ATTN: DTIC-DDA Cameron Station Alexandria, VA 22304-6145
1	Commander U.S. Army Materiel Command ATTN: AMCAM 5001 Eisenhower Ave. Alexandria, VA 22333-0001
1	Director U.S. Army Research Laboratory ATTN: AMSRL-D 2800 Powder Mill Rd. Adelphi, MD 20783-1145
1	Director U.S. Army Research Laboratory ATTN: AMSRL-OP-CI-A, Tech Publishing 2800 Powder Mill Rd. Adelphi, MD 20783-1145
2	Commander U.S. Army Armament Research, Development, and Engineering Center ATTN: SMCAR-IMI-I Picatinny Arsenal, NJ 07806-5000
2	Commander U.S. Army Armament Research, Development, and Engineering Center ATTN: SMCAR-TDC Picatinny Arsenal, NJ 07806-5000
1	Director Benet Weapons Laboratory U.S. Army Armament Research, Development, and Engineering Center ATTN: SMCAR-CCB-TL Watervliet, NY 12189-4050
(Unclass. only) 1	Commander U.S. Army Rock Island Arsenal ATTN: SMCRI-TL/Technical Library Rock Island, IL 61299-5000
1	Director U.S. Army Aviation Research and Technology Activity ATTN: SAVRT-R (Library) M/S 219-3 Ames Research Center Moffett Field, CA 94035-1000

No. of Copies	Organization
1	Commander U.S. Army Missile Command ATTN: AMSMI-RD-CS-R (DOC) Redstone Arsenal, AL 35898-5010
1	Commander U.S. Army Tank-Automotive Command ATTN: ASQNC-TAC-DIT (Technical Information Center) Warren, MI 48397-5000
1	Director U.S. Army TRADOC Analysis Command ATTN: ATRC-WSR White Sands Missile Range, NM 88002-5502
1	Commandant U.S. Army Field Artillery School ATTN: ATSF-CSI Ft. Sill, OK 73503-5000
(Class. only) 1	Commandant U.S. Army Infantry School ATTN: ATSH-CD (Security Mgr.) Fort Benning, GA 31905-5660
(Unclass. only) 1	Commandant U.S. Army Infantry School ATTN: ATSH-CD-CSO-OR Fort Benning, GA 31905-5660
1	WL/MNOI Eglin AFB, FL 32542-5000

Aberdeen Proving Ground

No. of Copies	Organization
2	Dir, USAMSAA ATTN: AMXSY-D AMXSY-MP, H. Cohen
1	Cdr, USATECOM ATTN: AMSTE-TC
1	Dir, ERDEC ATTN: SCBRD-RT
1	Cdr, CBDA ATTN: AMSCB-CI
1	Dir, USARL ATTN: AMSRL-SL-I
10	Dir, USARL ATTN: AMSRL-OP-CI-B (Tech Lib)

No. of Copies	Organization
1	Chairman DOD Explosives Safety Board Room 856-C Hoffman Bldg. 1 2461 Eisenhower Avenue Alexandria, VA 22331-0600
1	Headquarters U.S. Army Materiel Command ATTN: AMCICP-AD, M. Fisette 5001 Eisenhower Ave. Alexandria, VA 22333-0001
1	U.S. Army Ballistic Missile Defense Systems Command Advanced Technology Center P.O. Box 1500 Huntsville, AL 35807-3801
1	Department of the Army Office of the Product Manager 155mm Howitzer, M109A6, Paladin ATTN: SFAE-AR-HIP-IP, Mr. R. De Kleine Picatinny Arsenal, NJ 07806-5000
3	Project Manager Advanced Field Artillery System ATTN: SFAE-ASM-AF-E LTC D. Ellis T. Kuriata J. Shields Picatinny Arsenal, NJ 07801-5000
1	Project Manager Advanced Field Artillery System ATTN: SFAE-ASM-AF-Q, W. Warren Picatinny Arsenal, NJ 07801-5000
2	Commander Production Base Modernization Agency U.S. Army Armament Research, Development, and Engineering Center ATTN: AMSMC-PBM, A. Siklosi AMSMC-PBM-E, L. Laibson Picatinny Arsenal, NJ 07806-5000
4	PEO-Armaments Project Manager Tank Main Armament System ATTN: AMCPM-TMA AMCPM-TMA-105 AMCPM-TMA-120 AMCPM-TMA-AS, H. Yuen Picatinny Arsenal, NJ 07806-5000
5	Commander U.S. Army Armament Research, Development, and Engineering Center ATTN: SMCAR-CCD, D. Spring SMCAR-CCH-V, C. Mandala E. Fennell SMCAR-CCH-T, L. Rosendorf SMCAR-CCS Picatinny Arsenal, NJ 07806-5000
19	Commander U.S. Army Armament Research, Development, and Engineering Center ATTN: SMCAR-AEE, J. Lannon SMCAR-AEE-B, A. Beardell D. Downs S. Einstein S. Westley S. Bernstein J. Rutkowski B. Brodman P. O'Reilly R. Cirincione A. Grabowsky P. Hui J. O'Reilly SMCAR-AEE-WW, M. Mezger J. Pinto D. Wiegand P. Lu C. Hu SMCAR-AES, S. Kaplowitz Picatinny Arsenal, NJ 07806-5000
1	Commander U.S. Army Armament Research, Development and Engineering Center ATTN: SMCAR-HFM, E. Barrieres Picatinny Arsenal, NJ 07806-5000

No. of Copies | Organization

9 Commander
U.S. Army Armament Research, Development and Engineering Center
ATTN: SMCAR-FSA-T, M. Salsbury
SMCAR-FSA-F, LTC R. Riddle
SMCAR-FSC, G. Ferdinand
SMCAR-FS, T. Gora
SMCAR-FS-DH, J. Feneck
SMCAR-FSS-A, R. Kopman
B. Machek
L. Pinder
SMCAR-FSN-N, K. Chung
Picatinny Arsenal, NJ 07806-5000

3 Director
Benet Weapons Laboratories
ATTN: SMCAR-CCB-RA,
G.P. O'Hara
G.A. Pflegl
SMCAR-CCB-S, F. Heiser
Watervliet, NY 12189-4050

2 Commander
U.S. Army Research Office
ATTN: Technical Library
D. Mann
P.O. Box 12211
Research Triangle Park, NC 27709-2211

1 Commander, USACECOM
R&D Technical Library
ATTN: ASQNC-ELC-IS-L-R, Myer Center
Fort Monmouth, NJ 07703-5301

1 Commander
U.S. Army Harry Diamond Laboratory
ATTN: SLCHD-TA-L
2800 Powder Mill Rd.
Adelphi, MD 20783-1145

1 Commandant
U.S. Army Aviation School
ATTN: Aviation Agency
Fort Rucker, AL 36360

1 Program Manager
U.S. Tank-Automotive Command
ATTN: AMCPM-ABMS, T. Dean
Warren, MI 48092-2498

No. of Copies | Organization

1 Project Manager
U.S. Tank-Automotive Command
Fighting Vehicle Systems
ATTN: SFAE-ASM-BV
Warren, MI 48397-5000

1 Project Manager, Abrams Tank System
ATTN: SFAE-ASM-AB
Warren, MI 48397-5000

1 Director
HQ, TRAC RPD
ATTN: ATCD-MA
Fort Monroe, VA 23651-5143

2 Director
U.S. Army Materials Technology Laboratory
ATTN: SLCMT-ATL (2 cps)
Watertown, MA 02172-0001

1 Commander
U.S. Army Belvoir Research and Development Center
ATTN: STRBE-WC
Fort Belvoir, VA 22060-5006

1 Director
U.S. Army TRAC-Ft. Lee
ATTN: ATRC-L, Mr. Cameron
Fort Lee, VA 23801-6140

1 Commandant
U.S. Army Command and General Staff College
Fort Leavenworth, KS 66027

1 Commandant
U.S. Army Special Warfare School
ATTN: Rev and Trng Lit Div
Fort Bragg, NC 28307

1 Commander
Radford Army Ammunition Plant
ATTN: SMCAR-QA/HI LIB
Radford, VA 24141-0298

No. of Copies	Organization
1	Commander U.S. Army Foreign Science and Technology Center ATTN: AMXST-MC-3 220 Seventh Street, NE Charlottesville, VA 22901-5396
2	Commandant U.S. Army Field Artillery Center and School ATTN: ATSF-CO-MW, E. Dublisky ATSF-CN, P. Gross Ft. Sill, OK 73503-5600
1	Commandant U.S. Army Armor School ATTN: ATZK-CD-MS, M. Falkovitch Armor Agency Fort Knox, KY 40121-5215
2	Commander Naval Sea Systems Command ATTN: SEA 62R SEA 64 Washington, DC 20362-5101
1	Commander Naval Air Systems Command ATTN: AIR-954-Tech Library Washington, DC 20360
4	Commander Naval Research Laboratory ATTN: Technical Library Code 4410, K. Kailasanate J. Boris E. Oran Washington, DC 20375-5000
1	Office of Naval Research ATTN: Code 473, R.S. Miller 800 N. Quincy Street Arlington, VA 22217-9999
1	Office of Naval Technology ATTN: ONT-213, D. Siegel 800 N. Quincy St. Arlington, VA 22217-5000

No. of Copies	Organization
4	Commander Naval Surface Warfare Center ATTN: Code 730 Code R-13, R. Bernecker H. Sandusky Silver Spring, MD 20903-5000
7	Commander Naval Surface Warfare Center ATTN: T.C. Smith K. Rice S. Mitchell S. Peters J. Consaga C. Gotzmer Technical Library Indian Head, MD 20640-5000
5	Commander Naval Surface Warfare Center ATTN: Code G30, Code G32, Code G33, J.L. East T. Doran Code E23 Technical Library Dahlgren, VA 22448-5000
5	Commander Naval Air Warfare Center ATTN: Code 388, C.F. Price T. Boggs Code 3895, T. Parr R. Derr Information Science Division China Lake, CA 93555-6001
2	Commanding Officer Naval Underwater Systems Center ATTN: Code 5B331, R.S. Lazar Technical Library Newport, RI 02840
1	AFOSR/NA ATTN: J. Tishkoff Bolling AFB, D.C. 20332-6448
1	OLAC PL/TSTL ATTN: D. Shiplett Edwards AFB, CA 93523-5000

No. of Copies	Organization
3	AL/LSCF ATTN: J. Levine L. Quinn T. Edwards Edwards AFB, CA 93523-5000
1	WL/MNAA ATTN: B. Simpson Eglin AFB, FL 32542-5434
1	WL/MNME Energetic Materials Branch 2306 Perimeter Rd. STE 9 Eglin AFB, FL 32542-5910
1	WL/MNSH ATTN: R. Drabczuk Eglin AFB, FL 32542-5434
2	NASA Langley Research Center ATTN: M.S. 408, W. Scallion D. Witcofski Hampton, VA 23605
1	Central Intelligence Agency Office of the Central References Dissemination Branch Room GE-47, HQS Washington, DC 20502
1	Central Intelligence Agency ATTN: J. Backofen NHB, Room 5N01 Washington, DC 20505
1	SDIO/TNI ATTN: L.H. Caveny Pentagon Washington, DC 20301-7100
1	SDIO/DA ATTN: E. Gerry Pentagon Washington, DC 21301-7100
2	HQ DNA ATTN: D. Lewis A. Fahey 6801 Telegraph Rd. Alexandria, VA 22310-3398

No. of Copies	Organization
1	Director Sandia National Laboratories Energetic Materials & Fluid Mechanics Department, 1512 ATTN: M. Baer P.O. Box 5800 Albuquerque, NM 87185
1	Director Sandia National Laboratories Combustion Research Facility ATTN: R. Carling Livermore, CA 94551-0469
4	Director Lawrence Livermore National Laboratory ATTN: L-355, A. Buckingham G. Benedetti M. Finger L-324, M. Constantino P.O. Box 808 Livermore, CA 94550-0622
2	Director Los Alamos Scientific Lab ATTN: T3/D. Butler M. Division/B. Craig P.O. Box 1663 Los Alamos, NM 87544
2	Battelle Columbus Laboratories ATTN: TACTEC Library, J.N. Huggins V. Levin 505 King Avenue Columbus, OH 43201-2693
1	Battelle PNL ATTN: Mr. Mark Garnich P.O. Box 999 Richland, WA 99352
1	Institute of Gas Technology ATTN: D. Gidaspow 3424 S. State Street Chicago, IL 60616-3896

No. of Copies	Organization
1	Institute for Advanced Technology ATTN: T.M. Krehne The University of Texas of Austin 4030-2 W. Braker Lane Austin, TX 78759-5329
2	CPIA - JHU ATTN: Hary J. Hoffman T. Christian 10630 Little Patuxent Parkway Suite 202 Columbia, MD 21044-3200
1	Brigham Young University Department of Chemical Engineering ATTN: M. Beckstead Provo, UT 84601
1	Jet Propulsion Laboratory California Institute of Technology ATTN: L.D. Strand, MS 125/224 4800 Oak Grove Drive Pasadena, CA 91109
1	California Institute of Technology 204 Karman Lab Main Stop 301-46 ATTN: F.E.C. Culick 1201 E. California Street Pasadena, CA 91109
3	Georgia Institute of Technology School of Aerospace Engineering ATTN: B.T. Zim E. Price W.C. Strahle Atlanta, GA 30332
1	Massachusetts Institute of Technology Department of Mechanical Engineering ATTN: T. Toong 77 Massachusetts Avenue Cambridge, MA 02139-4307
2	University of Illinois Department of Mechanical/Industry Engineering ATTN: H. Krier R. Beddini 144 MEB; 1206 N. Green St. Urbana, IL 61801-2978

No. of Copies	Organization
1	University of Maryland ATTN: Dr. J.D. Anderson College Park, MD 20740
1	University of Massachusetts Department of Mechanical Engineering ATTN: K. Jakus Amherst, MA 01002-0014
1	University of Minnesota Department of Mechanical Engineering ATTN: E. Fletcher Minneapolis, MN 55414-3368
3	Pennsylvania State University Department of Mechanical Engineering ATTN: V. Yang K. Kuo C. Merkle University Park, PA 16802-7501
1	Rensselaer Polytechnic Institute Department of Mathematics Troy, NY 12181
1	Stevens Institute of Technology Davidson Laboratory ATTN: R. McAlevy III Castle Point Station Hoboken, NJ 07030-5907
1	Rutgers University Department of Mechanical and Aerospace Engineering ATTN: S. Temkin University Heights Campus New Brunswick, NJ 08903
1	University of Southern California Mechanical Engineering Department ATTN: 0HE200, M. Gerstein Los Angeles, CA 90089-5199
1	University of Utah Department of Chemical Engineering ATTN: A. Baer Salt Lake City, UT 84112-1194
1	Washington State University Department of Mechanical Engineering ATTN: C.T. Crowe Pullman, WA 99163-5201

No. of Copies	Organization
1	AFELM, The Rand Corporation ATTN: Library D 1700 Main Street Santa Monica, CA 90401-3297
1	Arrow Technology Associates, Inc. ATTN: W. Hathaway P.O. Box 4218 South Burlington, VT 05401-0042
3	AAI Corporation ATTN: J. Hebert J. Frankle D. Cleveland P.O. Box 126 Hunt Valley, MD 21030-0126
2	Alliant Techsystems, Inc. ATTN: R.E. Tompkins J. Kennedy 7225 Northland Dr. Brooklyn Park, MN 55428
1	AVCO Everett Research Laboratory ATTN: D. Stickler 2385 Revere Beach Parkway Everett, MA 02149-5936
1	General Applied Sciences Lab ATTN: J. Erdos 77 Raynor Ave. Ronkonkama, NY 11779-6649
1	General Electric Company Tactical System Department ATTN: J. Mandzy 100 Plastics Ave. Pittsfield, MA 01201-3698
1	IITRI ATTN: M.J. Klein 10 W. 35th Street Chicago, IL 60616-3799
4	Hercules, Inc. Radford Army Ammunition Plant ATTN: L. Gizzi D.A. Worrell W.J. Worrell C. Chandler Radford, VA 24141-0299

No. of Copies	Organization
2	Hercules, Inc. Allegheny Ballistics Laboratory ATTN: William B. Walkup Thomas F. Farabaugh P.O. Box 210 Rocket Center, WV 26726
1	Hercules, Inc. Aerospace ATTN: R. Cartwright 100 Howard Blvd. Kenville, NJ 07847
1	Hercules, Inc. Hercules Plaza ATTN: B.M. Riggleman Wilmington, DE 19894
1	MBR Research Inc. ATTN: Dr. Moshe Ben-Reuven 601 Ewing St., Suite C-22 Princeton, NJ 08540
1	Olin Corporation Badger Army Ammunition Plant ATTN: F.E. Wolf Baraboo, WI 53913
3	Olin Ordnance ATTN: E.J. Kirschke A.F. Gonzalez D.W. Worthington P.O. Box 222 St. Marks, FL 32355-0222
1	Olin Ordnance ATTN: H.A. McElroy 10101 9th Street, North St. Petersburg, FL 33716
1	Paul Gough Associates, Inc. ATTN: P.S. Gough 1048 South St. Portsmouth, NH 03801-5423
1	Physics International Library ATTN: H. Wayne Wampler P.O. Box 5010 San Leandro, CA 94577-0599

No. of Copies	Organization
2	Princeton Combustion Research Laboratories, Inc. ATTN: N. Mer N.A. Messina Princeton Corporate Plaza 11 Deerpark Dr., Bldg IV, Suite 119 Monmouth Junction, NJ 08852
3	Rockwell International Rocketdyne Division ATTN: BA08, J. Flanagan J. Gray R.B. Edelman 6633 Canoga Avenue Canoga Park, CA 91303-2703
2	Rockwell International Science Center ATTN: Dr. S. Chakravarthy Dr. S. Palaniswamy 1049 Camino Dos Rios P.O. Box 1085 Thousand Oaks, CA 91360
1	Southwest Research Institute ATTN: J.P. Riegel 6220 Culebra Road P.O. Drawer 28510 San Antonio, TX 78228-0510
1	Sverdrup Technology, Inc. ATTN: Dr. John Deur 2001 Aerospace Parkway Brook Park, OH 44142
3	Thiokol Corporation Elkton Division ATTN: R. Willer R. Biddle Tech Library P.O. Box 241 Elkton, MD 21921-0241
1	Veritay Technology, Inc. ATTN: E. Fisher 4845 Millersport Hwy. East Amherst, NY 14501-0305
1	Universal Propulsion Company ATTN: H.J. McSpadden 25401 North Central Ave. Phoenix, AZ 85027-7837

No. of Copies	Organization
1	SRI International Propulsion Sciences Division ATTN: Tech Library 333 Ravenwood Avenue Menlo Park, CA 94025-3493
	<u>Aberdeen Proving Ground</u>
1	Cdr, USACSTA ATTN: STECS-PO/R. Hendricksen